

1 The impact of regional climate model formulation and
2 resolution on simulated precipitation in Africa

3
4 Minchao Wu^{1,2}, Grigory Nikulin¹, Erik Kjellström^{1,3}, Danijel Belušić¹, Colin Jones⁴ and David
5 Lindstedt¹

6 Correspondence to: Minchao Wu (minchaowu.acd@gmail.com)

7
8 ¹Swedish Meteorological and Hydrological Institute, Folkborgsvägen 17, 60176 Norrköping,
9 Sweden

10 ²present affiliation, Department of Earth Sciences, Uppsala University, Uppsala, Sweden

11 ³Department of Meteorology and the Bolin Centre for Climate Research, Stockholm University,
12 10691, Stockholm, Sweden

13 ⁴National Centre for Atmospheric Science (NCAS), University of Leeds, Leeds, UK

14
15
16
17
18
19
20
21
22
23

Abstract

25 We investigate the impact of model formulation and horizontal resolution on the ability of
26 Regional Climate Models (RCMs) to simulate precipitation in Africa. Two RCMs (SMHI-RCA4
27 and HCLIM38-ALADIN) are utilized for downscaling the ERA-Interim reanalysis over Africa at
28 four different resolutions: 25, 50, 100 and 200km. In addition to the two RCMs, two different
29 parameter settings (configurations) of the same RCA4 are used. By contrasting different
30 downscaling experiments, it is found that model formulation has the primary control over many
31 aspects of the precipitation climatology in Africa. Patterns of spatial biases in seasonal mean
32 precipitation are mostly defined by model formulation while the magnitude of the biases is
33 controlled by resolution. In a similar way, the phase of the diurnal cycle in precipitation is
34 completely controlled by model formulation (convection scheme) while its amplitude is a
35 function of resolution. However, the impact of higher resolution on the time-mean climate is
36 mixed. An improvement in one region/season (e.g. reduction of dry biases) often corresponds to
37 a deterioration in another region/season (e.g. amplification of wet biases). At the same time,
38 higher resolution leads to a more realistic distribution of daily precipitation. Consequently, even
39 if the time-mean climate is not always greatly sensitive to resolution, the realism of the simulated
40 precipitation increases as resolution increases. Our results show that improvements in the ability
41 of RCMs to simulate precipitation in Africa compared to their driving reanalysis in many cases
42 are simply related to model formulation and not necessarily to higher resolution. Such model
43 formulation related improvements are strongly model dependent and can, in general, not be
44 considered as an added value of downscaling.

45

46

47 **Keywords:** RCA4, HCLIM, Resolution dependency, Added value, CORDEX-Africa

48

49

50

51

52

53

54

55

56

57

58

59

60

61

62

63

64

1 Introduction

66 Regional climate modeling is a dynamical downscaling method widely used for downscaling
67 coarse-scale global climate models (GCMs) to provide richer regional spatial information for
68 climate assessments and for impact and adaptation studies (Giorgi and Gao, 2018; Giorgi and
69 Mearns, 1991; Laprise, 2008; Rummukainen, 2010). It is well-established that regional climate
70 models (RCMs) are able to provide added value (understood as improved climatology) compared
71 to their driving GCMs. This includes better representation of regional and local weather and
72 climate features as a result of better capturing small-scale processes, including those influenced
73 by topography, coast lines and meso-scale atmospheric phenomena (Flato et al., 2013; Prein et
74 al., 2016). However, perceived added value from RCMs may have different causes and it may
75 not always be for the right reason where “right reason” would result from an improved
76 representation of regional processes at smaller scales. Such improvement leads to more accurate
77 simulations on local scales, and can, to some extent, also reduce large-scale GCM biases (Caron
78 et al., 2011; Diaconescu and Laprise, 2013; Sørland et al., 2018). Contrastingly, added value may
79 be attributed to different reasons, not directly related to higher resolution in RCMs but to
80 different model formulation in the RCMs and their driving GCMs. It is possible that the physics
81 of a RCM has been targeted for processes specific to the region it is being run for, giving it a
82 local advantage over GCMs that may have had their physics developed for global application.
83 However, it is questionable if improvements of such “downscaling” via physics can be
84 considered as an added value. In general, RCMs can either reduce or amplify GCM biases,
85 sometimes even changing their signs (Chan et al., 2013).

86 Issues as those mentioned above, have raised substantial concerns among regional climate
87 modelers (e.g., Castro, 2005; Xue et al., 2014). It has been pointed out that understanding of the
88 added value remains challenging. It would become even more complicated taking into account
89 the effects of different realizations, such as the size of domain, lateral boundary conditions,
90 geographical location, model resolution and its internal variability (Di Luca et al., 2015; Hong
91 and Kanamitsu, 2014; Rummukainen, 2016). All the above factors potentially influence RCM
92 simulations leading to different interpretations of the downscaling effects, therefore the
93 robustness of added value. For example, it was shown that over the Alps, downscaling with
94 multiple RCMs at increasing resolutions in general is able to provide a more realistic
95 precipitation pattern than the forcing GCMs, and it is regarded as added values from RCMs
96 (Giorgi et al., 2016; Torma et al., 2015). Similarly, Lucas-Picher et al (2017) found added value
97 over the Rocky Mountains, another region with strong topographic influence on hydrological
98 processes. However, the results are not unambiguous and sometimes limited added value is
99 found when comparing to the forcing data (e.g. Wang and Kotamarthi, 2014) over North
100 America. This implies that the understanding of downscaling effects is context-dependent and
101 one should carefully interpret GCM and RCM simulations in order to detect robust added value.
102 Africa is foreseen to be vulnerable to future climate change, which early on inspired efforts to
103 employ RCMs for impact and adaptation studies (e.g. Challinor et al., 2007). Further to previous
104 coordinated downscaling activities over Africa as for example the African Monsoon
105 Multidisciplinary Analyses (AMMA) (Van der Linden and Mitchell, 2009), the Coordinated
106 Regional climate Downscaling Experiment (CORDEX) provides a large ensemble of RCM
107 projections for Africa (Giorgi et al., 2009; Jones et al., 2011). All CORDEX RCMs follow a

108 common experiment protocol including a predefined domain at 50km resolution and common
109 output variables and format that facilitates assessment of projected climate changes in Africa.
110 Under this framework, RCMs at 50km horizontal resolution are found to have the capability of
111 providing added value in representing African climatological features compared to their forcing
112 GCMs, which generally have the resolution coarser than 100km (Dosio et al., 2015;
113 Moufouma-Okia and Jones, 2015; Nikulin et al., 2012).
114 However, a number of common challenges to accurately simulate precipitation climatology in
115 Africa have also been identified for the RCMs. Individual RCMs may exhibit substantial biases
116 in different aspects of the precipitation climatology as seasonal mean (Endris et al., 2013;
117 Kalognomou et al., 2013; Kim et al., 2014; Shongwe et al., 2015; Tamoffo et al., 2019), annual
118 cycle (Favre et al., 2016; Kisembe et al., 2019), onset and cessation of the rainy season
119 (Akinsanola and Ogunjobi, 2017; Gboganiyi et al., 2014), number of wet days and their intensity
120 (Klutse et al., 2016). At the same time, most of these studies found that such biases often
121 strongly depend on region and season. A RCM with a substantial bias in one region and/or
122 season may accurately simulate precipitation in other regions and seasons. It was also found that
123 the multi-model ensemble usually outperforms individual RCMs but it is a result of the
124 cancelation of opposite-signed biases in different RCMs.
125 A number of possible explanations for such RCM precipitation-related biases in Africa were
126 suggested as for example: different convection schemes (see discussion in Kalognomou et al.,
127 2013), land-atmosphere coupling (e.g. Sylla et al., 2013b) and biases in moisture transport
128 (Tamoffo et al., 2019). However, most of the CORDEX-Africa studies are still descriptive and
129 process-based evaluation studies like Tamoffo et al. (2019) are mostly lacking. An additional

130 barrier for more process-based evaluation studies is that the CORDEX requires atmospheric
131 variables at three pressure levels (850, 500 and 200mb) to be provided that seriously limits
132 evaluation of large-scale and regional circulation (e.g. jet streams) and moisture transport in the
133 troposphere.

134 Another common problem for almost all RCMs in Africa is the phase of the diurnal cycle of
135 precipitation. The majority of RCMs simulate maximum precipitation intensity around local
136 noon that is too early compared to late afternoon or even late evening maximum evident in
137 observations (Nikulin et al., 2012). This deficiency of the RCMs is related to the convective
138 parameterization used and some convection schemes, as for example the Kain–Fritsch (KF), may
139 outperform others, producing a more realistic diurnal cycle (Nikulin et al., 2012).

140 All the above deficiencies of the RCMs show that higher resolution does not necessarily lead to a
141 better performance of the RCMs in terms of precipitation climatology in Africa. It is also not
142 always clear if differences between the CORDEX Africa RCMs and their driving GCMs are
143 related to higher RCM resolution or to RCM internal formulation, or to the combination of both.
144 A thorough understanding of such differences and of the added value of the CORDEX-Africa
145 RCMs is necessary for robust regional assessments of future climate change and its impacts in
146 Africa.

147 In this study, we aim to separate the impact of model formulation and resolution on the ability of
148 RCMs to simulate precipitation in Africa. We conduct a series of sensitivity, reanalysis-driven
149 experiments by applying two different RCMs, one of them in two different configurations, at
150 four horizontal resolutions. Contrasting the different experiments allow us to separate the impact

151 of model formulation and resolution. We present an overview and the first results of the
152 experiments conducted and leave in-depth detailed process studies for different regions to
153 forthcoming papers.

154

2 Methods and Data

155

2.1 The Regional Climate Models

156 2.1.1 RCA4
157 The Rossby Centre Atmosphere regional climate model - RCA (Jones et al., 2004; Kjellström et
158 al., 2005; Räisänen et al., 2004; Rummukainen et al., 2001; Samuelsson et al., 2011) is based on
159 the numerical weather prediction model HIRLAM (Undén et al. 2002). To improve model
160 transferability, the latest fourth generation of RCA, RCA4, has a number of modifications for
161 specific physical parameterizations. This includes the modification of convective scheme based
162 on Bechtold-Kain-Fritsch scheme (Bechtold et al., 2001) with revised calculation of convective
163 available potential energy (CAPE) profile according to Jiao and Jones (2008), and the
164 introduction of turbulent kinetic energy (TKE) scheme (Lenderink and Holtslag, 2004). The
165 RCA4 model has been applied in many regions worldwide, among them Europe (Kjellström et
166 al., 2016, 2018; Kotlarski et al., 2015), the Arctic (Berg et al., 2013; Koenigk et al., 2015; Zhang
167 et al., 2014), Africa (Nikulin et al., 2018; Wu et al., 2016), South America (Collazo et al., 2018;
168 Wu et al., 2017), South-East (Tangang et al., 2018) and South Asia (Iqbal et al., 2017; Rana et
169 al., 2020).

170 RCA4 has three configurations used for CORDEX simulations that are available through the
171 Earth System Grid Federation (ESGF). They are named (so called RCM version) as v1 (Europe,
172 Arctic, Africa, Southeast Asia, Central and North America), v2 (South Asia) and v3 (South
173 America) and differ in some domain-specific re-tuning. In this study we also include a new
174 configuration - v4. The RCA4-v4 is based on RCA4-v1 but with a change in one parameter
175 leading to reduced turbulent mixing in stable situations (especially momentum mixing). Such
176 change in the parameter was applied to reduce a prominent dry bias found in the RCA4-v1
177 CORDEX Africa simulations over Central Africa ([Wu et al. 2016; Tamoffo et al. 2019](#)). Using
178 two parameter settings of RCA4 allows us to examine how sensitive our results are to such small
179 tuning of the same RCM.

180 2.1.2 HCLIM

181 HARMONIE-Climate (HCLIM) is a regional climate modelling system designed for a range of
182 horizontal resolutions from tens of kilometers to convection permitting scales of 1-3km (Belušić
183 et al., 2019; Lindstedt et al., 2015). It is based on the ALADIN-HIRLAM numerical weather
184 prediction system (Belušić et al., 2019; Bengtsson et al., 2017; Termonia et al., 2018). The
185 HCLIM system includes three atmospheric physics packages AROME, ALARO and ALADIN,
186 which are designed for different horizontal resolutions. The ALADIN model configuration used
187 in this study employs the hydrostatic ARPEGE-ALADIN dynamical core (Temperton et al.,
188 2001), a mass-flux scheme based on moisture convergence closure for parameterizing deep
189 convection (Bougeault, 1985), and SURFEX as the surface scheme (Masson et al., 2013). All
190 details about the version of HCLIM used in this study (HCLIM38), and its applications over

191 different regions can be found in (Belušić et al., 2019). We note that HCLIM38-ALADIN used in
192 the study is not the same model as ALADIN-Climate used in CORDEX (Daniel et al., 2019). We
193 refer to HCLIM38-ALADIN as HCLIM-ALADIN hereafter.

194

2.2 Experimental design

195 To investigate the response of both RCA4 and HCLIM-ALADIN to horizontal resolution, we
196 conduct a set of sensitivity experiments driven by the ERA-Interim reanalysis (denoted as
197 ERAINT hereafter; Dee et al., 2011) at four different resolutions. These resolutions are 1.76,
198 0.88, 0.44 and 0.22° for RCA4 with the rotated coordinate system and 200, 100, 50 and 25km for
199 HCLIM-ALADIN with the Lambert Conformal projection. The 0.44° or 50km resolution is
200 recommended by the CORDEX experiment design and used in the CORDEX-Africa ensemble.
201 Hereafter, the resolution in kilometers is used unless otherwise specified.

202 There are two approaches to set up a RCM experiment with simulations at different resolutions.
203 The first approach is to use the same full domain (including the relaxation zone) for all
204 simulations at different resolutions. Size of the full domain is defined by the coarsest resolution
205 in the experiment (200km in our case). A benefit of such experiment setup is a consistent lateral
206 boundary forcing for all simulations, given the same full domain. However, an unnecessary large
207 full domain for resolutions finer than 200km (i.e. 100, 50 and 25km) leads to larger RCM
208 internal variability (IV) compared to simulations at the same resolutions but with a minimum
209 size full domain. Computational demands at the finer resolutions are also higher in the case of
210 the large full domain. The second approach is to use different (minimum) full domains for
211 different resolutions defined only by size of the active domain (the same for all resolutions) and a

212 necessary relaxation zone (smaller in km for higher resolution). An advantage of this approach is
213 less IV and less computational demand for high resolution simulations while a shortcoming is
214 inconsistent lateral boundary forcing (different size of the full domain). We decided to use the
215 second approach with the minimum size of the full domain (less IV and computational demand),
216 although we note that a perfect experiment has to include both approaches, if resources allow.

217 The setup of the simulations at the four resolutions is identical apart from the timestep (adjusted
218 to ensure numerical simulation stability) and the size of the full computational domain with the
219 relaxation zone (see Table 1). The relaxation zone has 8 grid-points in all directions and
220 increases (in km) at coarser resolution while the interior CORDEX-Africa domain is the same.

221 As mentioned above, larger size of the computational domain at coarser resolution in our
222 experiment setup may have a potential impact on the simulated climatology leading to larger IV
223 developed by the RCMs and weaker constraints on the ERAINT forcing. As a simple test for
224 domain-dependent RCM IV we perform an additional experiment with RCA4 at 0.88° resolution
225 taking the full computational domain from the 1.76° RCA4 simulation. Indeed, for the
226 1981-2010 climatology, seasonal mean precipitation differences between the two experiments
227 can reach up to 1.25 mm/day (up to 25%) at a few individual grid boxes, often at the edges of the
228 tropical rain belt, although in general stay below 0.5 mm/day (not shown). Seasonal mean
229 temperature also differs with up to 1.25°C regionally (not shown). We do not focus on this single
230 additional sensitivity experiment in the study. A full set of simulations with the same full domain
231 for all RCMs and resolutions is necessary for robust conclusions.

232 Another source of IV in RCMs is related to different initialisation or starting time (e.g.
233 Lucas-Picher et al., 2008; Sanchez-Gomez and Somot, 2018). We perform two additional
234 experiments in order to see how different initialisation time impacts the IV in the RCMs. Both
235 RCA4-v1 and ALADIN at 50km were initialised on 1st January 1980 instead of 1st January
236 1979 as for all other simulations in the study. It was found that the impact of the different starting
237 time is much smaller than the impact of the larger domain. For both seasonal mean precipitation
238 and temperature, differences between the experiments are small over the African continent, in
239 general, less than 0.5 mm/day for precipitation and 0.25°C for temperature (not shown). Similar
240 to the domain-dependent sensitivity experiment above, we do not focus on these two additional
241 initialisation sensitivity experiments in the study. A full investigation of the initialisation-related
242 RCM IV needs generation of a larger (up to 10 members) ensemble for all RCMs and
243 resolutions.

244 We note that in general, both regional models - RCA and HCLIM-ALADIN were developed to
245 operate at a range of tens of km resolution and their performance at 100 and especially at 200km
246 may not be optimal. A potential caveat here is that very few RCM physical parameterisations are
247 automatically scaled to run at very coarse resolution. Thus, RCM deficiencies at the coarser
248 resolutions may be partly related to the lack of model retuning. We think that such
249 coarse-resolution simulations are a useful supplement to simulations at a RCM comfortable
250 resolution zone and help us to understand RCM behaviour without additional,
251 resolution-dependent tuning. All simulations are conducted without spectral nudging similar to
252 the CORDEX-Africa RCMs (Nikulin et al., 2012) allowing the RCMs to develop its own

253 climatology as much as possible. Analysis is done for the CORDEX-Africa domain shown in
254 Fig. 1.

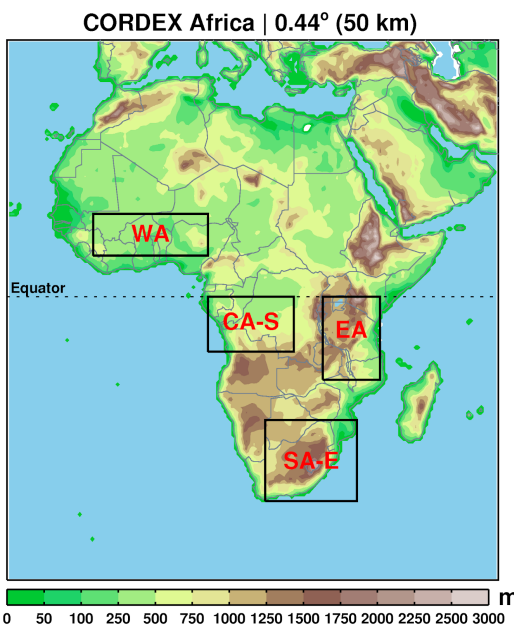
255 The difference between a RCM and its driving GCM can, in general, be attributed to three
256 sources, namely: i) different resolution, ii) different physical formulation and iii) artifacts of the
257 one-way nesting approach including size of the RCM domain and application of spectral nudging
258 (e.g. Scinocca et al., 2016). The RCA4 0.88° simulations and the HCLIM-ALADIN 100km one
259 represent a slight upscaling of ERAINT (about 0.7° or about 77km at the Equator) and we refer
260 to them as “no added value experiment” (NAVE). No resolution-dependent added value of the
261 RCMs is expected for these NAVE simulations and all differences between the RCMs and their
262 driving ERAINT are attributed to different physical formulations and to the artifacts of the one
263 way nesting. Spectral nudging is not used in our experiment and the one way nesting term is
264 basically reduced to domain configuration. In contrast, if spectral nudging is used, technical
265 aspects of the nudging (e.g. which wavelengths should be nudged and at what altitudes) also
266 contribute to the one way nesting term. In practice, it is not straightforward (if possible at all) to
267 separate the impact of different physical formulation and artifacts of the one-way nesting
268 approach. Hereafter, we use “RCM formulation” as a term that includes both RCM physical
269 formulation and domain-dependent RCM configuration (e.g. size of the full domain).

270 Table 1. The full domain configuration and time step for the RCA4 and HCLIM-ALADIN
271 simulations. The full domain includes the 8 grid point relaxation zone.

Experiment name	Horizontal resolution (deg. / km)	Domain size (lon \times lat)	Geographical area (deg.)		Time step (sec)
			South	North	
RCA4-v* 1.76°	1.76°	66 \times 67	-60.5, 55.66	-38.06, 76.34	1200

RCA4-v* 0.88°	0.88°	126 × 121	-54.78, 50.82	-33.22, 76.78	1200
RCA4-v* 0.44°	0.44°	222 × 222	-50.16, 47.08	-29.04, 68.20	1200
RCA4-v* 0.22°	0.22°	406 × 422	-48.07, 44.55	-26.95, 62.15	600
HCLIM-ALADIN 200km	200 km	80 × 90	-58.34, 56.71	-46.98, 82.98	1800
HCLIM-ALADIN 100km	100 km	128 × 150	-53.89, 51.70	-37.01, 73.01	1800
HCLIM-ALADIN 50km	50 km	240 × 270	-51.56, 48.98	-35.85, 71.85	1200
HCLIM-ALADIN 25km	25 km	450 × 512	-50.43, 47.73	-33.64, 69.64	600

272
273



274 **Figure 1** Topography (m) for the CORDEX-Africa domain in RCA4 at 50km resolution. Boxes indicate
275 the four subregions used for spatially averaged analysis: West Africa (WA), East Africa (EA), the
276 southern Central Africa (CA-S), and eastern southern Africa (SA-E).

277

2.3 Observations and reanalysis

278 Observational datasets in Africa, in general, agree well for large-scale climate features but can
279 deviate substantially at regional and local scales (Fekete et al., 2004; Gruber et al., 2000; Nikulin

280 et al., 2012). To take into account the observational uncertainties, we utilize a number of gridded
281 precipitation datasets. They include three gauged-based datasets: the Global Precipitation
282 Climatology Centre, GPCC, version 7 (Schneider et al., 2014), the Climate Research Unit
283 Time-Series, CRU TS, version 3.23 (Harris et al., 2014), and University of Delaware, UDEL,
284 version 4.01 (Legates and Willmott, 1990). All these three datasets are at 0.5° horizontal
285 resolution. For the evaluation of precipitation extremes and diurnal cycle simulated by RCMs,
286 we utilize a satellite-based precipitation dataset from the Tropical Rainfall Measuring Mission,
287 TRMM 3B42 version 7 (Huffman et al., 2007), which is at 0.25° horizontal resolution and
288 3-hourly temporal resolution. The TRMM product starts in 1998 and for evaluation of
289 precipitation extremes and diurnal cycle we use a shorter period (1998-2010) in contrast to
290 1981-2010 used for evaluation of seasonal means and annual cycle. We also note that the TRMM
291 3B42-v7 precipitation product provides satellite-based precipitation estimates adjusted by the
292 GPCC gauge-based precipitation. This means that monthly mean TRMM 3B42 and GPCC
293 precipitation are almost the same if remapped to the same resolution or averaged over a region.
294 ERAINT as the driving reanalysis is also used for analysis. In contrast to climate models,
295 ERAINT precipitation is a short term forecast product and there are several ways to derive
296 ERAINT precipitation (e.g. different spin-up, base time and forecast steps) that can lead to
297 different precipitation estimates (Dee et al. 2011). ERAINT precipitation for this study is derived
298 by the simplest method, without spinup as in some of the previous studies (Dosio et al., 2015;
299 Moufouma-Okia and Jones, 2015; Nikulin et al., 2012): 3-hourly precipitation uses the base
300 times 00/12 and forecast steps 3/6/9/12 hours, while daily precipitation uses base times 00/12
301 and forecast steps of 12 hours. The RCMs and ERAINT represent 3-hourly mean precipitation

302 for the 00:00-03:00, 03:00-06:00, ... 21:00-00:00 intervals while TRMM precipitation averages
303 represent approximately the 22:30–01:30, 01:30–04:30, ... 19:30–22:30 UTC intervals.

304

2.4 Methods

305 The coarsest resolution 200km is used as a reference resolution for spatial maps. The
306 higher-resolution simulations are aggregated to the 200km grid by the first-order conservative
307 remapping method (Jones, 1999). In this way we expect that the difference among the aggregated
308 simulations at common resolution should mainly be caused by the different treatment for
309 fine-scale processes (Di Luca et al., 2012). For the regional analysis, such as the analysis of
310 annual cycle, diurnal cycle and daily precipitation intensity, we focus on four subregions,
311 presenting different climate zones in Africa: West Africa ($10^{\circ}\text{W}\sim10^{\circ}\text{E}$, $7.5^{\circ}\text{N}\sim15^{\circ}\text{N}$), East
312 Africa ($30^{\circ}\text{E}\sim40^{\circ}\text{E}$, $15^{\circ}\text{S}\sim0^{\circ}\text{S}$), the southern Central Africa ($10^{\circ}\text{E}\sim25^{\circ}\text{E}$, $10^{\circ}\text{S}\sim0^{\circ}\text{S}$), and the
313 eastern South Africa ($20^{\circ}\text{E}\sim36^{\circ}\text{E}$, $35^{\circ}\text{S}\sim22^{\circ}\text{S}$) as defined in Fig. 1. The period 1981-2010 is
314 used for the analysis in this study, unless otherwise specified.

315

3 Results and Discussion

316

3.1 Seasonal mean

317 In the boreal summer defined here as July-September (JAS), the tropical rain belt (TRB)
318 associated with the intertropical convergence zone (ITCZ) is positioned to its northernmost
319 location with the maximum precipitation north of the Equator (Fig. 2a). CRU, UDEL and GPCC
320 aggregated to the 200km resolution, generally agree well with each other, with only slight local
321 differences (Fig. 2a-c). ERAINT overestimates precipitation over Central Africa and along the

322 Guinea Coast while underestimates it over West Africa, north of the Guinea Coast (Fig. 2d). All
323 RCA4-v1 simulations have a pronounced dry bias (Fig. 2e-h) that spatially almost coincides with
324 the wet bias in ERAINT and increases at coarser resolution (Fig2e-f). RCA4-v4 shows a similar
325 pattern compared to RCA4-v1 but substantially reduces the dry bias over Central Africa at all
326 four resolutions (Fig. 2i-l). For both configurations of RCA4, the smallest dry bias is found at the
327 highest 25km resolution. At the same time, an overestimation of precipitation north of the central
328 dry-bias region becomes more pronounced, especially for RCA4-v4. HCLIM-ALADIN, in
329 general, shows some similarities to RCA4 with a pronounced dry bias in West and Central Africa
330 at 200km that is strongly reduced with increasing resolution. However, a wet bias emerges on the
331 northern flank of the rain belt at 50 and 25km. For JAS there is a common tendency for both
332 RCMs to generate more precipitation at higher resolution leading to a reduction of the dry biases
333 over Central Africa. Such bias reduction may be considered as a resolution-related improvement.
334 However, the RCM simulations clearly show that the added value of higher resolution can be
335 region-dependent. An improvement of the simulated precipitation climatology over one region
336 corresponds to deterioration of the climatology over another region. Moufouma-Okia and Jones
337 (2015) found a mixed response to resolution in simulated seasonal mean precipitation over West
338 Africa. Their RCM simulations at 50 and 12km bear a great deal of similarity with each other
339 while a simulation at 25km shows wetter conditions in the Sahel and drier ones near the coastal
340 area in the south (see their Fig. 8). In contrast, Panitz et al. (2014) found almost no difference in
341 seasonal rainfall over West Africa between two RCM simulations at 50 and 25km. We conclude
342 that for both RCA4 and HCLIM-ALADIN, spatial bias patterns are similar and more related to
343 model formulation while magnitude of biases are more sensitive to resolution. For example, the

344 sign of the bias pattern in our no added value RCM simulations at 100km in JAS (Fig. 2f, j, n) is
345 almost opposite to the sign of the bias pattern in the driving ERAINT (Fig. 2d).

346

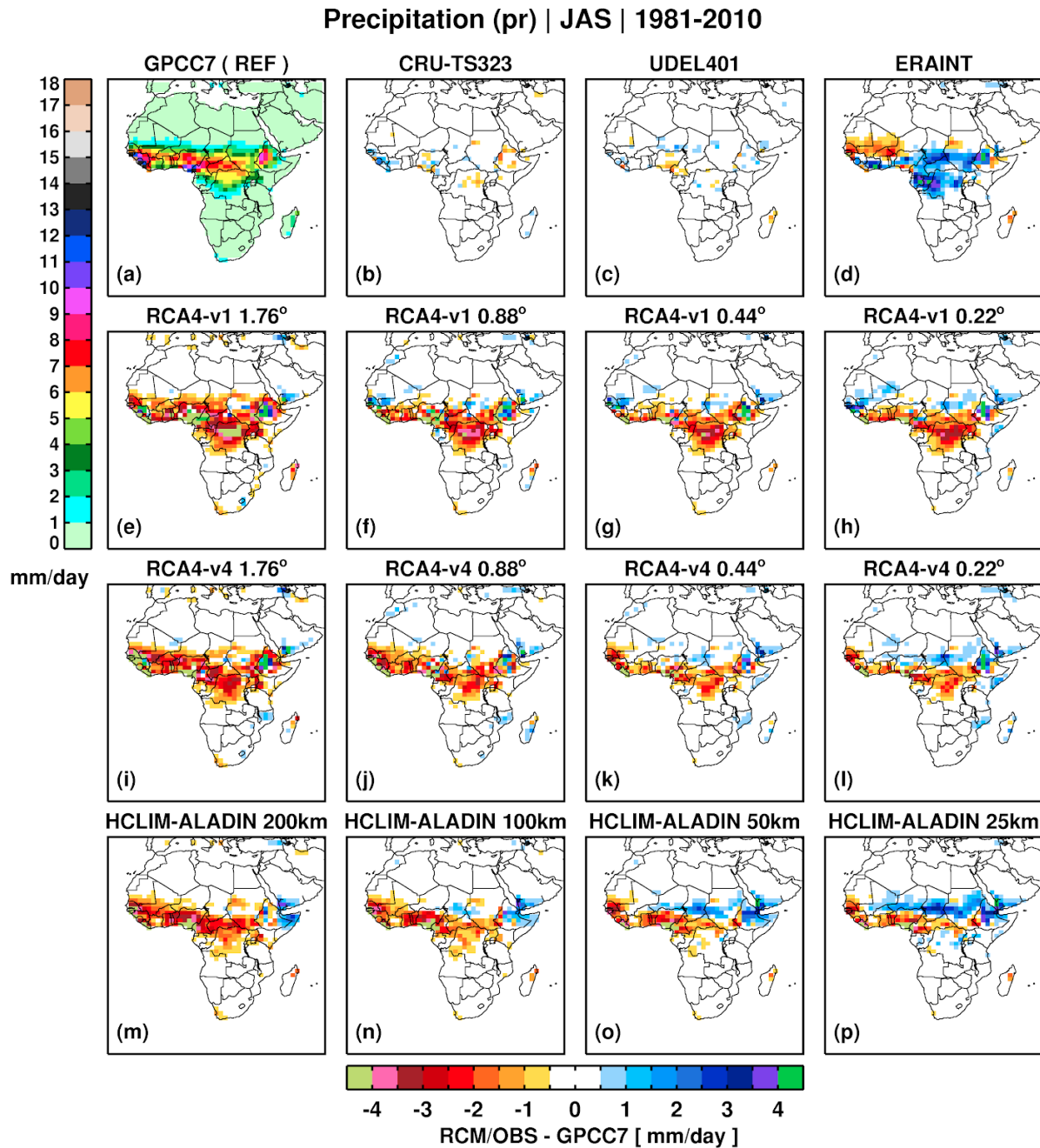


Figure 2. GPCC7 mean JAS precipitation for 1981–2010 and differences compared to GPCC7 in (b-d) the other gridded observations, (e-h) the RCA4-v1, (i-l) RCA4-v4 and (m-p) HCLIM-ALADIN simulations. All data sets are aggregated to the coarsest 200km grid.

350

351 In boreal winter (December–February, DJF), the TRB migrates to its most southerly position

352 covering the latitudes from southern to Central Africa, with the maximum over southern tropical

353 Africa and Madagascar (Fig. 3a). Similar to JAS, observational uncertainties are generally small

354 in DJF and there is a pronounced wet bias in ERAINT over Central Africa (Fig. 3d). At 25 and

355 50km RCA4-v1 has a dipole bias pattern with an underestimation of rainfall over Central Africa

356 and an overestimation over southern Africa. At 200km there is a pronounced deterioration in the

357 simulated rainfall: a strong dry bias appears along the eastern coast and Madagascar while the

358 wet bias is amplified over large parts of southwestern Africa. At 25 and 50km RCA4-v4 shows a

359 large-scale dipole bias pattern similar in some degree to RCA4-v1. The RCA4-v4 biases are

360 smaller than the RCA4-v1 ones showing an impact of the re-tuning (reducing mixing in the

361 boundary layer). The behaviour of RCA4-v4 at coarser resolution is also similar to RCA4-v1. A

362 similar strong dry bias is emerging along the eastern coast at 200km. However, in contrast to

363 RCA4-v1, the dry bias over the Democratic Republic of Congo almost completely disappears at

364 both 100 and 200km. HCLIM-ALADIN simulates almost the same bias pattern at all resolutions,

365 strongly underestimating rainfall over southeastern Africa and overestimating it over the Guinea

366 Coast, parts of central Africa and southern Africa. There is a tendency to an increase in

367 precipitation with higher resolution in HCLIM-ALADIN: the wet biases are amplified and the

368 dry biases are reduced. Both RCA4 and HCLIM-ALADIN show a common feature -

369 intensification of the dry bias along the eastern coast of Africa at 200km. Even if both RCMs

370 have this dry bias in common, there are also differences showing the importance of model

371 formulation. HCLIM-ALADIN has about the same bias pattern at all four resolutions while the

372 RCA4 bias pattern substantially changes across the resolutions. Such resolution dependency in
373 RCA4 may be related to the fact that RCA4 is based on a limited area model and not developed
374 to operate at 100-200km resolution. Contrastingly, HCLIM-ALADIN that is based on a global
375 model shows more consistent results even at 100-200km resolution. This indicates that
376 HCLIM-ALADIN parameterisations may be better suited to work also at coarser resolution.
377 Although, we also note that the resolution dependency of the RCA4 bias pattern over southern
378 Africa is similar to that found for the CMIP5 GCMs (Munday and Washington, 2018). They
379 show that the GCMs with the coarsest resolution and respectively the lowest topography have the
380 wettest bias over the Kalahari basin and the driest bias over the southeast Africa coast, the
381 Mozambique Channel and Madagascar. Such a bias pattern is related to a smoother barrier to
382 northeasterly moisture transport from the Indian Ocean that penetrates across the high
383 topography of Tanzania and Malawi into subtropical southern Africa. However, in our analysis,
384 HCLIM-ALADIN does not show such resolution-related dependency. In general, similar to JAS,
385 the added value of higher resolution in DJF is region-dependent: with higher resolution biases
386 are reduced over one region but amplified over another.
387

Precipitation (pr) | DJF | 1981-2010

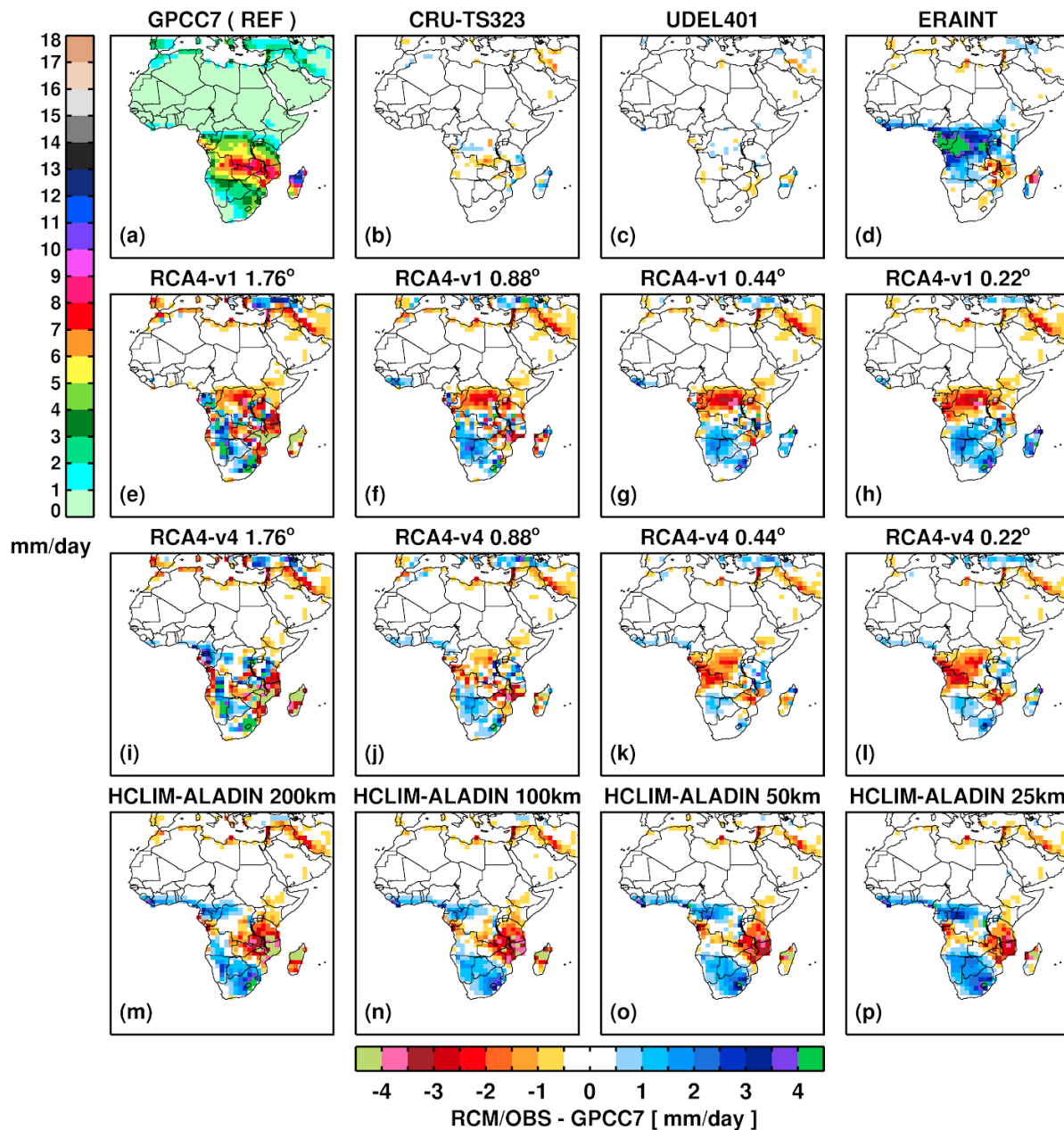


Figure 3. As Fig. 2, but for DJF.

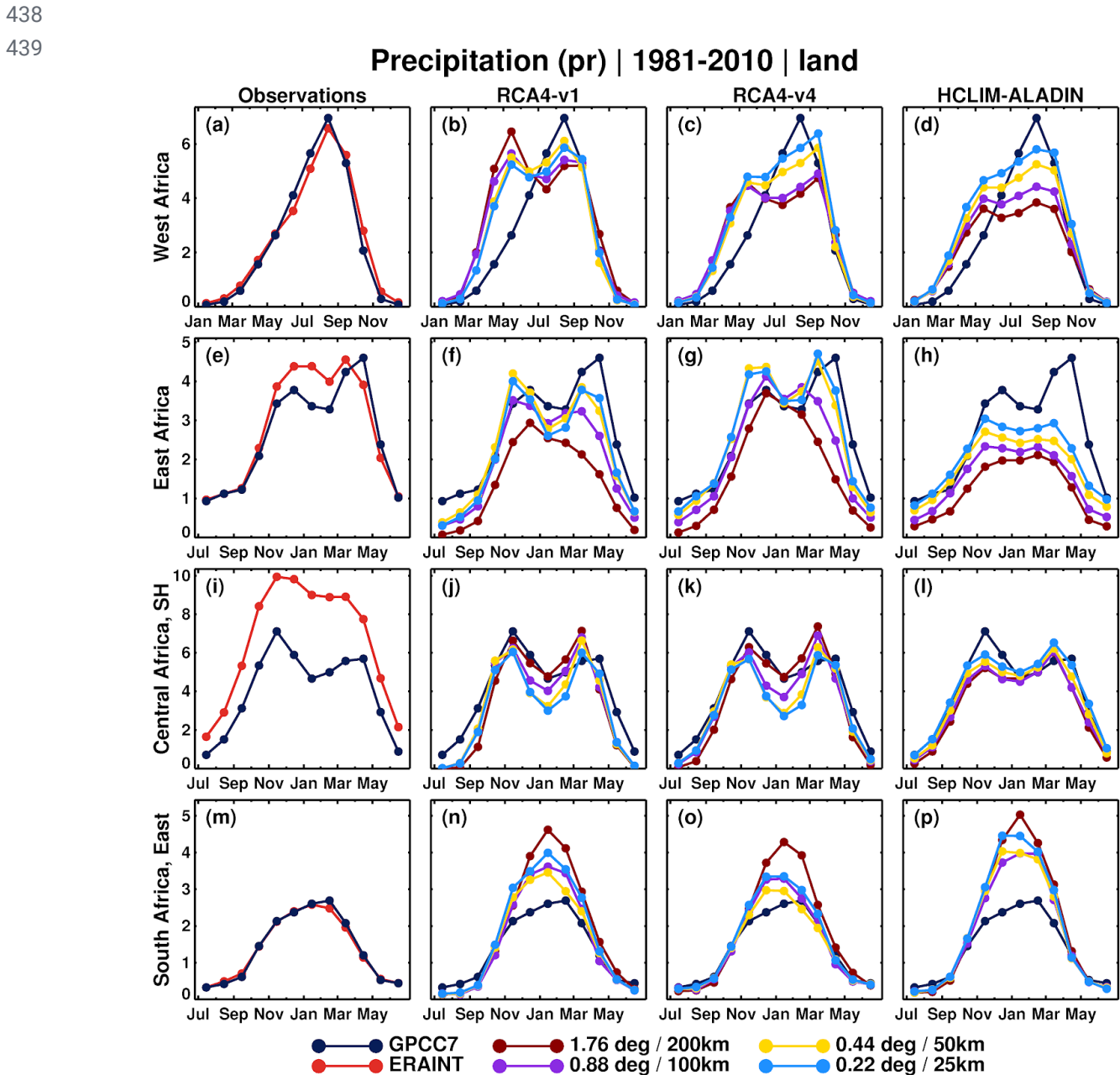
3.2 Annual cycle

391 The annual cycle of precipitation over the four subregions is shown in Fig. 4. The observed
 392 annual cycle of precipitation over West Africa depicts the West African Monsoon (WAM)

393 rainfall, with maximum precipitation in August (Fig. 4a). All observational datasets (CRU and
394 UDEL are not shown) and ERAINT agree well with each other with only a small
395 underestimation of rainfall by ERAINT in June-August. In contrast to the observations,
396 RCA4-v1 has a bimodal annual cycle with a too early onset of the rainy season (Fig. 4b). The
397 simulated rainfall is overestimated in March-May, underestimated in July-August during the
398 active WAM period and is well in line with the observations during the cessation of the WAM
399 rainfall in September-November. RCA4-v4 shows a similar behaviour but the first rainfall peak
400 in May is reduced and the annual cycle has a more unimodal shape (Fig. 4c). HCLIM-ALADIN,
401 in general, shows similar features as both configurations of RCA4, although has more
402 similarities with RCA4-v4 (Fig. 4d). The too early onset of the rainy season is a common
403 problem for many RCMs reported by Nikulin et al., (2012). Our results show that this is not
404 dependent on resolution but instead related to model formulation. Higher resolution reduces the
405 wet bias during the onset of the rainy season for RCA-v1, has no impact for RCA-v4 and
406 amplifies the wet bias in HCLIM-ALADIN. Nevertheless, the impact of higher resolution is
407 more consistent during the rainy season. Increasing resolution tends to increase monsoon rainfall
408 for both RCMs, resulting in smaller dry biases and a pattern closer to the unimodal one in the
409 observations. Eastern and Central Africa have a bimodal annual cycle of rainfall with two peaks
410 around November and May (Fig. 4e,i). GPCC, CRU and UDEL (both not shown) agree well on
411 the phase and magnitude of the annual cycle for both subregions. ERAINT has a weaker
412 bimodality overestimating precipitation in December-February over Eastern Africa and all year
413 round over Central Africa with the largest wet bias during October-April. Both configurations of
414 RCA4 fail to reproduce the bimodal annual cycle in Eastern Africa at 200km underestimating

415 precipitation all year round and showing a single rainfall peak in December (Fig. 4j,k).
416 Increasing resolution reduces the dry bias and leads to an improvement in the shape of the annual
417 cycle. The bimodal shape begins to appear at 100km and becomes much closer to the observation
418 at 50 and 25km. Despite some mixed dry and wet biases in different seasons, the 25 and 50km
419 RCA4 simulations show the best agreement with the observations. In contrast to RCA4,
420 HCLIM-ALADIN simulates the unimodal annual cycle at all four resolutions and some signs of
421 bimodality only appear at 25km (Fig. 4h). Similar to RCA4, increasing resolution leads to an
422 increase in precipitation in HCLIM-ALADIN, although a dry bias is a prominent feature from
423 November to May in all HCLIM-ALADIN simulations. For Central Africa, the bimodality of the
424 annual cycle is well reproduced by both RCMs at all resolutions (Fig. 4j-l). HCLIM-ALADIN
425 maintains similar behavior to that in Eastern Africa, although the difference in precipitation
426 across the resolutions is small (Fig. 4l). On the other hand, for both configurations of RCA4 in
427 Central Africa, increasing resolution leads to decreasing precipitation during the rainy seasons,
428 especially in January. Both RCMs strongly reduce the ERAINT wet bias even in the NAVE at
429 100km. Such improvement indicates that model formulation plays a more important role than
430 resolution over Central Africa. For the eastern Southern Africa, the annual cycle of precipitation
431 is unimodal with its maximum during austral summer (Fig. 4m). Similar to West Africa,
432 uncertainties between observational datasets and reanalysis are small. RCA4 in general
433 overestimates rainfall during the rainy season with the largest wet bias at 200km. Surprisingly,
434 the simulated rainfall is almost the same at 25 and 100km while the smallest bias is found at
435 50km for both RCA4 configurations. HCLIM-ALADIN also overestimates precipitation during

436 the rainy season at all four resolutions (Fig. 4p). However, the smallest wet bias in the
 437 HCLIM-ALADIN simulations is found at 50 and 100km.



440 **Figure 4.** Annual cycle of precipitation over the four subregions for 1981-2010 in observations/ERAINT
 441 and as simulated by RCA4 and HCLIM-ALADIN at the four different resolutions. Only land grid boxes
 442 are used for averaging over the subregions. Units are mm/day.

443
 444
 445

3.3 Diurnal cycle

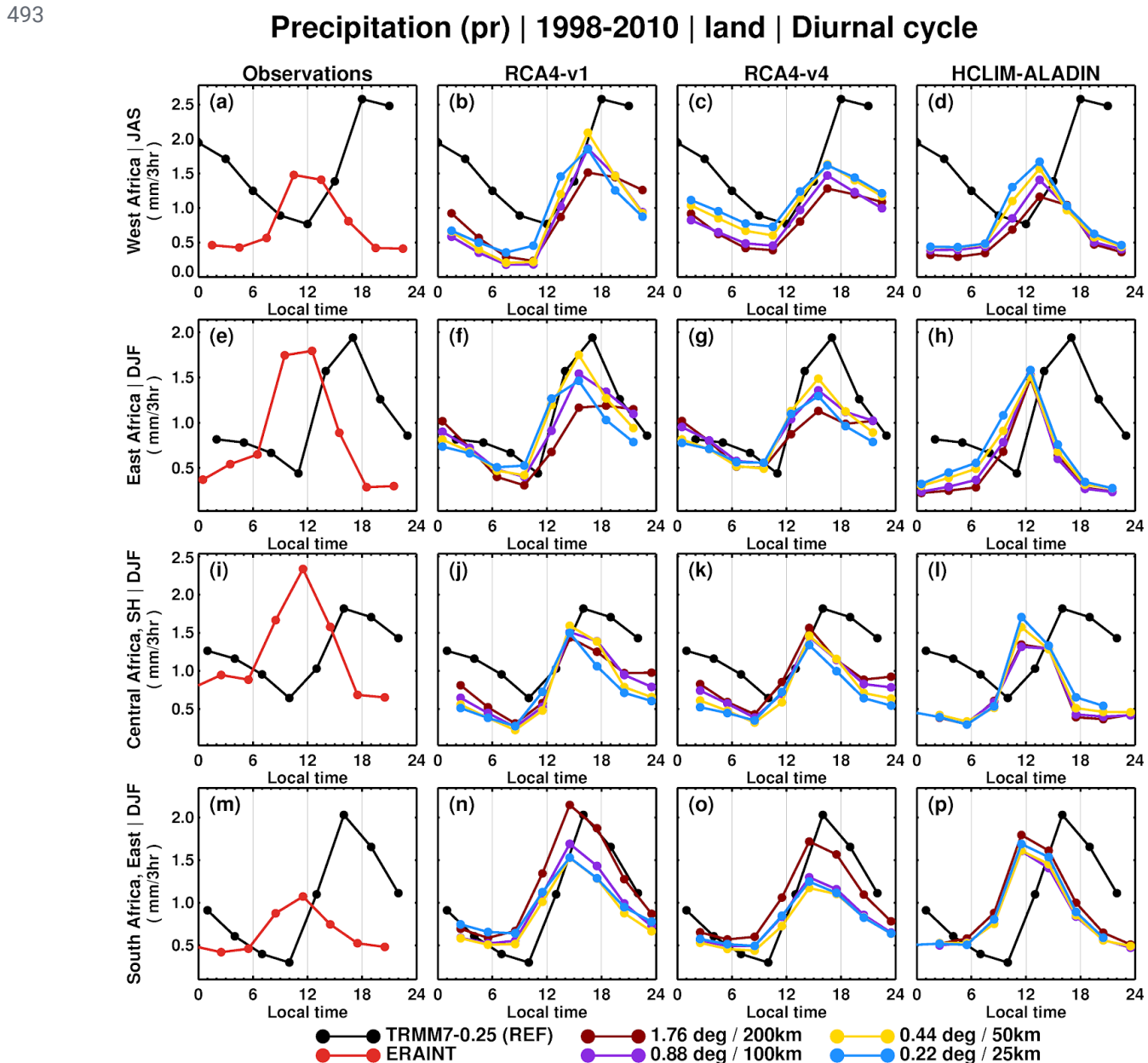
447 The diurnal cycle is a prominent feature of forced atmospheric variability with a strong impact
 448 on regional- and local-scale thermal and hydrological regimes. The diurnal cycle of precipitation
 449 in the tropics is well documented and includes a late afternoon/evening maximum over land (Dai
 450 et al., 2007). However, it is still a common challenge for GCMs (Dai, 2006; e.g. Dai and
 451 Trenberth, 2004; Dirmeyer et al., 2012), RCMs (e.g. Da Rocha et al., 2009; Jeong et al., 2011;
 452 Nikulin et al., 2012) and reanalyses (Nikulin et al., 2012) to accurately represent the diurnal
 453 cycle of precipitation.

454 The TRMM diurnal cycle of precipitation generally shows an increase of rainfall starting around
 455 noon with maximum reached at around 18:00 local solar time (LST) (Fig. 5). The ERAINT
 456 diurnal cycle is completely out of phase over all subregions with the occurrence of maximum
 457 precipitation intensity around local noon. A common feature of ERAINT is an overestimation of
 458 precipitation around local noon and an underestimation during the rest of the day.

459 HCLIM-ALADIN shows exactly the same behaviour as ERAINT. Both configurations of RCA4
 460 simulate the diurnal cycle of precipitation more accurately compared to ERAINT and
 461 HCLIM-ALADIN. The phase of the diurnal cycle, in general, is pretty well captured over all
 462 four subregions. In terms of precipitation intensity RCA4 underestimates rainfall from afternoon
 463 to morning over West (Fig. 5b,c) and Central Africa (Fig. 5j,k). Reducing mixing in the
 464 boundary layer results in flattening of the diurnal cycle over West Africa (Fig. 5b, c) while there
 465 are almost no changes over Central Africa (Fig. 5j, k). RCA4-v1 very well simulates the diurnal
 466 cycle over Eastern Africa with only some underestimation in early morning and afternoon (Fig.
 467 5f). RCA4-v4 improves rainfall intensity in early morning but at the same time shows a slightly

468 larger underestimation in afternoon than RCA4-v1 (Fig. 5g). Over Southern Africa the RCA4
469 simulations at 200km are the closest to the observation (Fig. 5n,o) while the simulations at
470 higher resolutions underestimate the amplitude of the diurnal cycle in the afternoon.
471 Figure 5 clearly shows that the phase of the diurnal cycle of precipitation in Africa does not
472 depend on resolution but instead depends on model formulation. Both ERAINT, with the Tiedtke
473 convection scheme (Tiedtke, 1989), and HCLIM-ALADIN with the Bougeault scheme
474 (Bougeault, 1985) trigger precipitation too early during the diurnal cycle while both
475 configurations of RCA4 with the same Kain–Fritsch (KF) scheme (Bechtold et al., 2001)
476 simulate much more realistic diurnal cycle. It has previously been shown that the KF scheme is
477 able to reproduce late afternoon rainfall peaks for the regions where moist convection is
478 governed by the local forcing, for example in the southeast US (Liang, 2004) and in the tropical
479 South America and Africa (e.g. Bechtold et al., 2004; Da Rocha et al., 2009). Nikulin et al.,
480 (2012) also found that a subset of RCMs that employ the KF scheme show an improved
481 representation of the phase of the diurnal cycle in Africa. Our results indicate that the impact of
482 resolution is only seen in the amplitude of the diurnal cycle. However, such impact is not
483 homogeneous across the subregions and the RCMs. For HCLIM-ALADIN, increasing resolution
484 leads to increasing rainfall intensity in all regions but southern Africa. RCA4 shows a similar
485 behaviour over West Africa, while there is a mixed response over Eastern and Central Africa.
486 These findings are in line with previous studies investigating resolution effects for GCMs (Covey
487 et al., 2016; Dirmeyer et al., 2012) and for RCMs (Walther et al., 2013). In coarser-scale models
488 (e.g. >10km), increasing resolution only leads to changes in the magnitude, but not in the phase
489 of the diurnal cycle of precipitation over land.

490 Nevertheless, studies conducting sensitivity experiments using resolutions finer than 10 km do
 491 find improvements in the representation of the phase (Dirmeyer et al., 2012; Sato et al., 2009;
 492 Walther et al., 2013).



494 **Figure 5.** Diurnal cycle of 3-hourly mean precipitation over the four subregions for 1998-2010 in
 495 observations/ERAINT and as simulated by RCA4 and HCLIM-ALADIN at the four different resolutions.
 496 Only land grid boxes are used for averaging over the subregions and only wet days with more than
 497 1mm/day are taken for estimations of the diurnal cycle.

498

3.4 Frequency and intensity of daily precipitation

500 Figure 6 shows the empirical probability density function (PDF) of daily precipitation intensities
501 over the four subregions. The TRMM7-0.25 dataset, aggregated to the common 1.76° resolution
502 (TRMM7-1.76), as expected has a shorter right tail with no precipitation intensities larger than
503 100 mm day^{-1} and higher frequency for lower intensities less than 25 mm day^{-1} (Fig. 6a,e,i,m).
504 The two TRMM7 PDFs provide reference bounds for datasets with resolution between 0.25° and
505 1.76° . However, uncertainties in gridded daily precipitation products in Africa are large (Sylla et
506 al., 2013a) and we take the TRMM bounds as an observational approximation focusing more on
507 differences in the simulated PDFs across the four resolutions. Over West, East and central Africa
508 ERAINT overestimates the frequency of low ($< 10 \text{ mm day}^{-1}$) and extremely high ($> 150 \text{ mm}$
509 day^{-1}) intensities while it underestimates the frequency of precipitation intensities in between
510 (Fig. 6a,e,i), especially over West Africa (Fig. 6a). In southern Africa (Fig. 6m) ERAINT
511 represents the frequency of daily mean precipitation more accurately compared to the other three
512 regions but shows almost no events with more than 150 mm day^{-1} in contrast to the observations.
513 Both RCMs, in general, have the same tendency to generate more higher-intensity precipitation
514 events with increasing resolution over all four subregions. In West Africa RCA4-v1 strongly
515 underestimates the frequency of intensities with more than 20 mm day^{-1} at 200, 100 and 50km
516 (Fig. 6b). A substantial improvement appears only at 25km where the right tail of the PDF
517 extends up to 250 mm day^{-1} , although the frequency of precipitation events from about 50 to 150
518 mm day^{-1} is still underestimated.
519 The RCA4-v4 configuration markedly reduces the RCA4-v1 biases and shows more realistic
520 PDFs at all four resolutions (Fig. 6c). The RCA4-v4 50km simulation generates precipitation

521 events up to 250 mm day⁻¹ strongly contrasting to the RCA4-v1 simulation at the same resolution
522 (no events for more than 100 mm day⁻¹). However, RCA4-v4 overestimates frequencies of high
523 intensities at 25km. Such sharp difference between two configurations of RCA4 at the same
524 resolution shows that model formulation also plays an important role for accurately reproducing
525 daily precipitation. Over West Africa all HCLIM-ALADIN simulations overestimates the
526 frequency of low precipitation intensities (less than 10 mm day⁻¹) and underestimates the
527 frequency of intensities in the range of 10-150 mm day⁻¹ (Fig. 6d). Similar to RCA4, higher
528 resolution leads to more high-intensity precipitation events in the HCLIM-ALADIN simulations.
529 However, RCA4 and HCLIM-ALADIN behave in a different way with increasing resolution.
530 Both RCMs change the PDFs by adding more higher-intensity precipitation events extending the
531 right-hand tail towards higher intensities. In addition, RCA4 also increases the frequency of
532 medium- and high-intensity events especially going from 50 to 25km. In eastern Africa both
533 RCA4 configurations reproduce the observed PDFs almost perfectly (Fig. 6f, g). All four
534 resolutions are located within the TRMM-1.76 and TRMM-0.25 boundaries and the coarsest and
535 finest resolutions coincide with the respective TRMM PDFs. Contrastingly, HCLIM-ALADIN
536 strongly underestimates the frequency of precipitation events with more than 20 mm day⁻¹ (Fig.
537 6h) over eastern Africa and even the highest 25km resolution is located below the coarse
538 TRMM-1.76 dataset. In central Africa both RCMs overestimate the occurrence of intensities less
539 than 20 mm day⁻¹ (Fig. 6j,k,l), especially HCLIM-ALADIN (Fig. 6l) and strongly underestimate
540 the frequency of higher-intensity events. The PDFs at all four resolutions for both RCMs are
541 located below the coarsest TRMM-1.76 PDF. We note that observational uncertainties in
542 precipitation are very large over central Africa and we should be careful in the interpretation of

543 Fig. 6j-l. Seasonal mean precipitation, for example, can differ by more than 50% across different
544 observational datasets (Washington et al., 2013). Additionally, the TRMM dataset is scaled by
545 the gauge-based GPCC precipitation product while almost no long-term gauges are available in
546 the region (Nikulin et al., 2012). In southern Africa RCA4 and HCLIM-ALADIN simulate the
547 precipitation PDFs quite accurately (Fig. 6n-p). An interesting detail is that the 50km
548 HCLIM-ALADIN simulation shows higher frequency for intensities in the range of 50 to about
549 200 mm/day than the 25km simulation.

550 In general, we see the improvement of simulated daily rainfall intensities with increasing
551 resolution across the African continent. There are many studies showing a similar resolution-
552 dependent improvement over both complex terrains and flat regions (e.g. Chan et al., 2013;
553 Huang et al., 2016; Lindstedt et al., 2015; Olsson et al., 2015; Prein et al., 2016; Torma et al.,
554 2015; Walther et al., 2013). Our results are in agreement with the above studies and confirm
555 increasing fidelity of simulated daily rainfall intensities with increasing resolution.

556

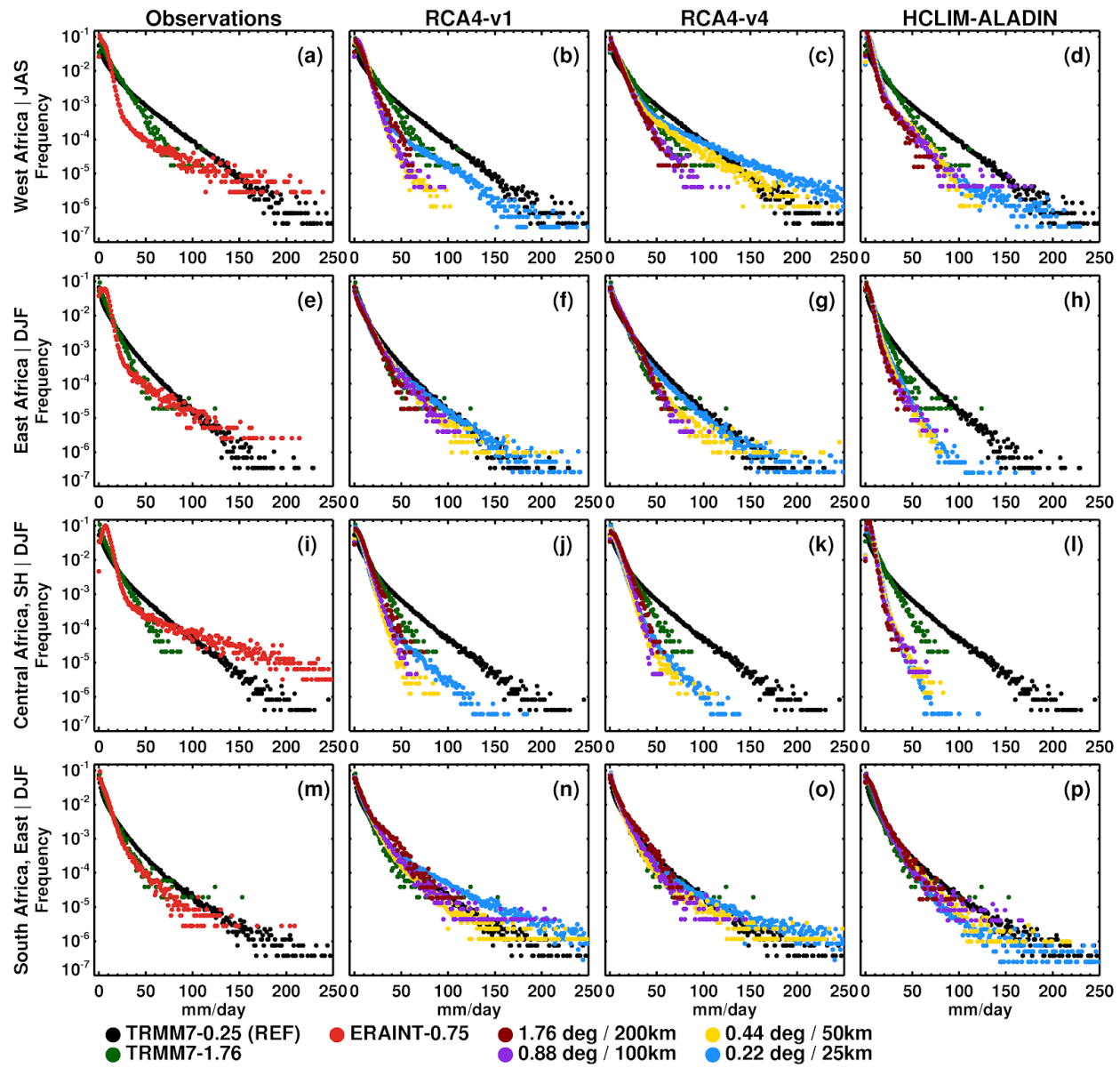
557

558

559

560

Precipitation (pr) | 1998-2010 | land | PDF



562
 563 **Figure 6.** Probability distribution function of daily precipitation intensities pooled over the four subregions
 564 for 1998-2010 in observations/ERAINT and as simulated by RCA4 and HCLIM-ALADIN at the four
 565 different resolutions. TRMM7-1.76 represents TRMM7-0.25 aggregated from its native 0.25° resolution
 566 to 1.76° . A base-10 log scale is used for the frequency axis and the first bin ($0-1 \text{ mm day}^{-1}$) is divided by
 567 10. Only land grid boxes are used for pooling over the subregions and the season is different for the
 568 different regions.
 569

4 Summary and Conclusion

572 In this study we have investigated the impact of model formulation and spatial resolution on
573 simulated precipitation in Africa. A series of sensitivity, ERA-Interim reanalysis-driven
574 experiments, were conducted by applying two different RCMs (RCA4 and HCLIM-ALADIN) at
575 four resolutions (about 25, 50, 100 and 200km). The 100km experiment, at resolution a bit
576 coarser than the driving ERA-Interim reanalysis, by default does not provide any
577 resolution-dependent added value while such added value is expected for the 50 and 25km
578 experiments. The 200km experiment is about 3 times upscaling of ERAINT to resolution of
579 many CMIP5 GCMs and should only be considered as a supplementary experiment since RCMs
580 do not aim to operate at such coarse resolution. In addition to the two different RCMs, the
581 standard CORDEX configuration of RCA4 is supplemented by another configuration with
582 reduced mixing in the boundary layer. Such configuration was developed to deal with a strong
583 dry bias of RCA4 in Central Africa. Contrasting the two different RCMs and the two different
584 configurations of the same RCM at the four different resolutions allow us to separate the impact
585 of model formulation and resolution on simulated rainfall in Africa.

586 Even if the results often depend on region and season and a clear separation of the impact of
587 model formulation and resolution is not always straightforward, we found that model
588 formulation has the primary control over many aspects of the precipitation climatology in Africa.
589 The 100km NAVE shows that patterns of spatial biases in seasonal mean precipitation are mostly
590 defined by model formulation. These patterns are very different between the driving ERAINT
591 and RCMs, sometimes even with opposite signs, exemplified by the two configurations of RCA4

592 in JAS (Fig. 1e-l). Resolution in general controls the magnitude of biases and for both RCA4 and
593 HCLIM-ALADIN higher resolution usually leads to an increase in precipitation amount while
594 preserving large-scale bias patterns. A side effect of such an increase in precipitation amount is
595 that an improvement in one region (e.g. reduction of dry biases) often corresponds to a
596 deterioration in another region (amplification of wet biases) as for HCLIM-ALADIN in JAS
597 (Fig. 1m-p). Nevertheless, on average the smallest biases in seasonal means are found for the
598 simulations at 50 and 25km resolution.

599 The impact of model formulation and resolution on the annual cycle of precipitation is mixed
600 and strongly depends on region and season. For example, in both West and Central Africa the
601 shape of the annual cycle for the 100km NAVE is different from ERAINT. However, the impact
602 of model formulation is opposite between these two regions. In West Africa both RCMs
603 deteriorate the ERAINT annual cycle by simulating a too early onset of the rainy season. In
604 contrast, over Central Africa, both models improve the ERAINT annual cycle by reducing a
605 strong wet bias and changing the unimodal annual cycle to a bimodal one similar to the
606 observations. The impact of resolution can also be different. In West and East Africa, higher
607 resolution (50 and 25km) leads to an improvement in the annual cycle (more realistic shape and
608 smaller biases). In contrast, over Central Africa, the 25km RCA4 simulations show the largest
609 biases while the HCLIM-ALADIN simulations at all four resolutions are almost similar. In
610 general, it is difficult to conclude on a common impact of model formulation and resolution on
611 the annual cycle.

612 The phase of the diurnal cycle in Africa is completely controlled by model formulation
613 (convection scheme) while its amplitude is a function of resolution. Both ERAINT and

614 HCLIM-ALADIN show a too early precipitation maximum around noon while RCA4 simulates
615 a much more realistic diurnal cycle with an evening maximum. Higher resolution does not
616 change the phase of the diurnal cycle but its amplitude, although the impact of resolution on the
617 amplitude is mixed across the four subregions and time of the day.

618 A pronounced and well known impact of higher resolution on daily precipitation intensities is a
619 more realistic distribution of daily precipitation. Our results also show that higher resolution, in
620 general, improves the distribution of daily precipitation. This includes reduced overestimation of
621 the number of days with low precipitation intensities and reduced underestimation of the number
622 of days with high intensities. The latter results in extending the right-hand tail of the distribution
623 towards higher intensities similar to observations. This also means that at higher resolutions the
624 time-mean climate (e.g. seasonal mean and annual cycle) is made up of more realistic
625 underpinning daily precipitation than at lower resolutions. It is also worth emphasizing that if
626 low resolution models are not able to simulate high rainfall days then it will be difficult for them
627 to say anything robust about projected climate changes in high rainfall events. However,
628 regionally, model formulation can also play an important role in the distribution of daily
629 precipitation. For example, in West Africa the 50km RCA4-v4 configuration with reduced
630 mixing in the boundary layer shows a remarkable improvement in the shape of the PDF (Fig. 6c)
631 compared to the standard RCA4-v1 configuration at the same resolution (Fig 6b). Moreover, the
632 RCA4-v4 configuration at 50km shows almost the same PDF as RCA4-v1 at 25km. Such
633 contrast indicates that for daily precipitation intensities model formulation can have the same
634 impact as doubled resolution.

635 Improvements in simulated precipitation in high-resolution RCMs relative to coarse-scale GCMs
636 are often attributed as being a resolution-dependent added value of downscaling. Our results
637 show that for Africa improvements are not always related to higher resolution but also to
638 different model formulation between the RCMs and their driving reanalysis. A common
639 framework for quantifying added value of downscaling is to evaluate some aspects of the climate
640 in high-resolution RCM simulations and in their coarse-resolution driving reanalysis or GCMs
641 over a historical period (Di Luca et al., 2015; e.g. Hong and Kanamitsu, 2014; Rummukainen,
642 2016). If the RCM simulations show smaller biases compared to reference observations than the
643 driving GCMs, one can conclude that RCMs provide an added value and vice versa. However,
644 such a framework does not separate the impact of different model formulation between RCMs
645 and their driving GCMs and higher resolution in the RCM simulations. Our results indicate that
646 improvements in RCM simulations may simply be related to different model formulation and not
647 necessarily to higher resolution. In general, model formulation related improvements cannot be
648 considered as an added value of downscaling as such improvements are strongly model
649 dependent and cannot be generalised. However, such formulation-related and region-specific
650 improvements from RCMs could in principle be also used in GCMs.
651 Within the commonly used RCM evaluation framework, e.g. the CORDEX evaluation
652 experiment, it is not straightforward, if possible at all, to isolate the impact of model formulation
653 and resolution in RCM simulations. We show that running RCMs at about the same resolution as
654 a driving reanalysis (e.g. ERAINT at about 80km or ERA5 at about 30km) helps to separate the
655 impacts of model formulation and higher resolution in dynamical downscaling. We propose that
656 such a simple additional experiment can be an integral part of the RCM evaluation framework in

657 order to elucidate the added value of downscaling. In our study, as the first step, we focus only
658 on precipitation that has large relevance for climate change impact studies. As the next step, we
659 foresee similar studies looking also at other variables and especially at processes and drivers
660 relevant for regional climate.

661 Moreover, the same NAVE framework can be used for quantifying the added value in
662 RCM-based future climate projections. For this, one needs to downscale GCMs at their native
663 resolution in addition to the standard CORDEX resolutions (25 or 50km). The RCM projections
664 at the native GCM resolution serve as the NAVE in the climate change context. A potential
665 caveat, already mentioned in our study, is that RCMs are generally developed and tuned to
666 operate at resolution of tens of km. “Downscaling” a GCM at its native resolution, for example
667 150 or 200km, may lead to artefacts related to a lack of RCM retuning for coarser resolution.
668 Nevertheless, more and more GCMs, for example in CMIP6, have resolution finer than 100km that
669 allows application of the NAVE.

670

671

672

673

674

675

676

677

Code availability

678 The analysis is done in MATLAB and IDL and codes can be provided by request as they are but
679 without support on implementing them in another computing environment.

680

Data availability

681 The ERA-Interim reanalysis is available at <https://apps.ecmwf.int/datasets/>, the GPCC dataset is
682 available at <https://www.dwd.de/EN/ourservices/gpcc/gpcc.html>, the CRU dataset is available at
683 <https://catalogue.ceda.ac.uk/uuid/5dca9487dc614711a3a933e44a933ad3>, the UDEL dataset is
684 available at http://climate.geog.udel.edu/~climate/html_pages/download.html, the TRMM
685 dataset is available at <https://pmm.nasa.gov/data-access/downloads/trmm>. The RCA4 and
686 HCLIM-ALADIN data can be provided by request.
687

Author contribution

688 MW performed RCA4 simulations and all the analysis and wrote the initial draft. GN developed
689 the experiment design and provided guidance for the analysis. EK and GN revised the initial
690 draft. CJ is responsible for setting up the new RCA4 configuration (v4). DB and DL are
691 responsible for performing the HCLIM-ALADIN simulations over Africa. All the authors
692 contributed with discussions and revisions.
693

Conflict of interest

694 There is no conflict of interest in this study.
695

Acknowledgements

696 We thank one anonymous reviewer and John Scinocca for their very helpful comments.
697 This work was done with support from the FRACTAL (www.fractal.org.za) and AfriCultuReS
698 (<http://africancultures.eu/>) projects. FRACTAL is part of the multi-consortia Future Climate for
699 Africa (FCFA) programme - jointly funded by the UK's Department for International
700 Development (DFID) and the Natural Environment Research Council (NERC). AfriCultuReS
701 has received funding from the European Union's Horizon 2020 research and innovation
702 programme under grant agreement No 774652. The authors thank the European Centre for
703 Medium-Range Weather Forecasts (ECMWF), the Global Precipitation Climatology Centre
704 (GPCC), the British Atmospheric Data Centre (BADC), the University of East Anglia (UEA),

705 the University of Delaware and the Goddard Space Flight Center (GSFC) for providing data. All
706 simulations were conducted on the supercomputer in the National Supercomputer Centre,
707 Linköping, Sweden.

708

709

710

711

712

713

714

715

716

717

718

719

720

721

722

723

724

725

726

727

728

729

730

731

732

733

734

735

736

737

738

739

740

741

742

743

744

Reference

746 Akinsanola, A. A. and Ogunjobi, K. O.: Evaluation of present-day rainfall simulations over West
747 Africa in CORDEX regional climate models, *Environ. Earth Sci.*, 76(10), 366, 2017.

748 Bechtold, P., Bazile, E., Guichard, F., Mascart, P. and Richard, E.: A mass-flux convection
749 scheme for regional and global models, *Q.J Royal Met. Soc.*, 127(573), 869–886, 2001.

750 Bechtold, P., Chaboureau, J. P., Beljaars, A., Betts, K., Köhler, M., Miller, M. and Redelsperger,
751 J. L.: The simulation of the diurnal cycle of convective precipitation over land in a global model,
752 *Quarterly Journal of the Royal Meteorological Society*, (130), 3119–3137, 2004.

753 Belušić, D., de Vries, H., Dobler, A., Landgren, O., Lind, P., Lindstedt, D., Pedersen, R. A.,
754 Sánchez-Perrino, J. C., Toivonen, E., van Ulft, B. and Others: HCLIM38: A flexible regional
755 climate model applicable for different climate zones from coarse to convection permitting scales,
756 *Geoscientific Model Development Discussion*, doi:10.5194/gmd-2019-151, 2019.

757 Bengtsson, L., Andrae, U., Aspelien, T., Batrak, Y., Calvo, J., de Rooy, W., Gleeson, E.,
758 Hansen-Sass, B., Homleid, M., Hortal, M., Ivarsson, K.-I., Lenderink, G., Niemelä, S., Nielsen,
759 K. P., Onvlee, J., Rontu, L., Samuelsson, P., Muñoz, D. S., Subias, A., Tijm, S., Toll, V., Yang, X.
760 and Køltzow, M. Ø.: The HARMONIE–AROME Model Configuration in the ALADIN–HIRLAM
761 NWP System, *Mon. Weather Rev.*, 145(5), 1919–1935, 2017.

762 Berg, P., Döscher, R. and Koenigk, T.: Impacts of using spectral nudging on regional climate
763 model RCA4 simulations of the Arctic, *Geoscientific Model Development*, 6(3), 849–859, 2013.

764 Bougeault, P.: A Simple Parameterization of the Large-Scale Effects of Cumulus Convection,
765 *Mon. Weather Rev.*, 113(12), 2108–2121, 1985.

766 Caron, L.-P., Jones, C. G. and Winger, K.: Impact of resolution and downscaling technique in
767 simulating recent Atlantic tropical cyclone activity, *Clim. Dyn.*, 37(5), 869–892, 2011.

768 Castro, C. L.: Dynamical downscaling: Assessment of value retained and added using the
769 Regional Atmospheric Modeling System (RAMS), *J. Geophys. Res.*, 110(D5), 681, 2005.

770 Challinor, A., Wheeler, T., Garforth, C., Craufurd, P. and Kassam, A.: Assessing the vulnerability
771 of food crop systems in Africa to climate change, *Clim. Change*, 83(3), 381–399, 2007.

772 Chan, S. C., Kendon, E. J., Fowler, H. J., Blenkinsop, S., Ferro, C. A. T. and Stephenson, D. B.:
773 Does increasing the spatial resolution of a regional climate model improve the simulated daily
774 precipitation?, *Clim. Dyn.*, 41(5), 1475–1495, 2013.

775 Collazo, S., Lhotka, O., Rusticucci, M. and Kysel`y, J.: Capability of the SMHI-RCA4 RCM
776 driven by the ERA-Interim reanalysis to simulate heat waves in Argentina, *Int. J. Climatol.*,
777 38(1), 483–496, 2018.

778 Covey, C., Gleckler, P. J., Doutriaux, C., Williams, D. N., Dai, A., Fasullo, J., Trenberth, K. and
779 Berg, A.: Metrics for the Diurnal Cycle of Precipitation: Toward Routine Benchmarks for Climate

780 Models, *J. Clim.*, 29(12), 4461–4471, 2016.

781 Dai, A.: Precipitation Characteristics in Eighteen Coupled Climate Models, *J. Clim.*, 19(18),
782 4605–4630, 2006.

783 Dai, A. and Trenberth, K. E.: The Diurnal Cycle and Its Depiction in the Community Climate
784 System Model, *J. Clim.*, 17(5), 930–951, 2004.

785 Dai, A., Lin, X. and Hsu, K.-L.: The frequency, intensity, and diurnal cycle of precipitation in
786 surface and satellite observations over low- and mid-latitudes, *Clim. Dyn.*, 29(7), 727–744,
787 2007.

788 Daniel, M., Lemonsu, A., Déqué, M., Somot, S., Alias, A. and Masson, V.: Benefits of explicit
789 urban parameterization in regional climate modeling to study climate and city interactions, *Clim.*
790 *Dyn.*, 52(5), 2745–2764, 2019.

791 Da Rocha, R. P., Morales, C. A., Cuadra, S. V. and Ambrizzi, T.: Precipitation diurnal cycle and
792 summer climatology assessment over South America: An evaluation of Regional Climate Model
793 version 3 simulations, *Journal of Geophysical Research*, doi:10.1029/2008JD010212, 2009.

794 Dee, D. P., Uppala, S. M., Simmons, A. J., Berrisford, P., Poli, P., Kobayashi, S., Andrae, U.,
795 Balmaseda, M. A., Balsamo, G., Bauer, d. P. and Others: The ERA-Interim reanalysis:
796 Configuration and performance of the data assimilation system, *Quart. J. Roy. Meteor. Soc.*,
797 137(656), 553–597, 2011.

798 Diaconescu, E. P. and Laprise, R.: Can added value be expected in RCM-simulated large
799 scales?, *Clim. Dyn.*, 41(7), 1769–1800, 2013.

800 Di Luca, A., de Elía, R. and Laprise, R.: Potential for added value in precipitation simulated by
801 high-resolution nested Regional Climate Models and observations, *Clim. Dyn.*,
802 doi:10.1007/s00382-011-1068-3, 2012.

803 Di Luca, A., de Elía, R. and Laprise, R.: Challenges in the Quest for Added Value of Regional
804 Climate Dynamical Downscaling, *Current Climate Change Reports*, 1(1), 10–21, 2015.

805 Dirmeyer, P. A., Cash, B. A., Kinter, J. L., Jung, T., Marx, L., Satoh, M., Stan, C., Tomita, H.,
806 Towers, P., Wedi, N., Achuthavarier, D., Adams, J. M., Altshuler, E. L., Huang, B., Jin, E. K. and
807 Manganelli, J.: Simulating the diurnal cycle of rainfall in global climate models: resolution
808 versus parameterization, *Clim. Dyn.*, 39(1), 399–418, 2012.

809 Dosio, A., Panitz, H.-J., Schubert-Frisius, M. and Lüthi, D.: Dynamical downscaling of CMIP5
810 global circulation models over CORDEX-Africa with COSMO-CLM: evaluation over the present
811 climate and analysis of the added value, *Clim. Dyn.*, 44(9), 2637–2661, 2015.

812 Endris, H. S., Omondi, P., Jain, S., Lennard, C., Hewitson, B., Chang'a, L., Awange, J. L., Dosio,
813 A., Ketiem, P., Nikulin, G., Panitz, H.-J., Büchner, M., Stordal, F. and Tazalika, L.: Assessment of
814 the Performance of CORDEX Regional Climate Models in Simulating East African Rainfall, *J.*
815 *Clim.*, 26(21), 8453–8475, 2013.

816 Favre, A., Philippon, N., Pohl, B., Kalognomou, E.-A., Lennard, C., Hewitson, B., Nikulin, G.,

817 Dosio, A., Panitz, H.-J. and Cerezo-Mota, R.: Spatial distribution of precipitation annual cycles
818 over South Africa in 10 CORDEX regional climate model present-day simulations, *Clim. Dyn.*,
819 46(5), 1799–1818, 2016.

820 Fekete, B. M., Vörösmarty, C. J., Roads, J. O. and Willmott, C. J.: Uncertainties in Precipitation
821 and Their Impacts on Runoff Estimates, *J. Clim.*, 17(2), 294–304, 2004.

822 Flato, G., Marotzke, J., Abiodun, B., Braconnot, P., Chou, S. C., Collins, W., Cox, P., Driouech,
823 F., Emori, S., Eyring, V., Forest, C., Gleckler, P., Guilyardi, E., Jakob, C., Kattsov, V., Reason, C.
824 and Rummukainen, M.: Evaluation of Climate Models, *Climate Change 2013: The Physical
825 Science Basis. Contribution of Working Group I to the Fifth Assessment Report of the
826 Intergovernmental Panel on Climate Change*, 741–866, 2013.

827 Gbobaniyi, E., Sarr, A., Sylla, M. B., Diallo, I., Lennard, C., Dosio, A., Dhiédiou, A., Kamga, A.,
828 Klutse, N. A. B., Hewitson, B., Nikulin, G. and Lamptey, B.: Climatology, annual cycle and
829 interannual variability of precipitation and temperature in CORDEX simulations over West Africa,
830 *Int. J. Climatol.*, 34(7), 2241–2257, 2014.

831 Giorgi, F. and Gao, X.-J.: Regional earth system modeling: review and future directions,
832 *Atmospheric and Oceanic Science Letters*, 11(2), 189–197, 2018.

833 Giorgi, F. and Mearns, L. O.: Approaches to the simulation of regional climate change: A review,
834 *Rev. Geophys.*, 29(2), 191, 1991.

835 Giorgi, F., Jones, C., Asrar, G. R. and Others: Addressing climate information needs at the
836 regional level: the CORDEX framework, *WMO Bull.*, 58(3), 175, 2009.

837 Giorgi, F., Torma, C., Coppola, E., Ban, N., Schär, C. and Somot, S.: Enhanced summer
838 convective rainfall at Alpine high elevations in response to climate warming, *Nat. Geosci.*, 9(8),
839 584–589, 2016.

840 Gruber, A., Su, X., Kanamitsu, M. and Schemm, J.: The Comparison of Two Merged Rain
841 Gauge–Satellite Precipitation Datasets, *Bull. Am. Meteorol. Soc.*, 81(11), 2631–2644, 2000.

842 Harris, I., Jones, P. D., Osborn, T. J. and Lister, D. H.: Updated high-resolution grids of monthly
843 climatic observations--the CRU TS3. 10 Dataset, *Int. J. Climatol.*, 34(3), 623–642, 2014.

844 Hong, S. Y. and Kanamitsu, M.: Dynamical downscaling: Fundamental issues from an NWP
845 point of view and recommendations, *Asia-Pacific Journal of Atmospheric Sciences*, 50(1),
846 83–104, 2014.

847 Huang, X., Rhoades, A. M., Ullrich, P. A. and Zarzycki, C. M.: An evaluation of the
848 variable-resolution CESM for modeling California's climate, *Journal of Advances in Modeling
849 Earth Systems*, 8(1), 345–369, 2016.

850 Huffman, G. J., Bolvin, D. T., Nelkin, E. J., Wolff, D. B., Adler, R. F., Gu, G., Hong, Y., Bowman,
851 K. P. and Stocker, E. F.: The TRMM Multisatellite Precipitation Analysis (TMPA): Quasi-Global,
852 Multiyear, Combined-Sensor Precipitation Estimates at Fine Scales, *J. Hydrometeorol.*, 8(1),
853 38–55, 2007.

854 Iqbal, W., Syed, F. S., Sajjad, H., Nikulin, G., Kjellström, E. and Hannachi, A.: Mean climate and
855 representation of jet streams in the CORDEX South Asia simulations by the regional climate
856 model RCA4, *Theor. Appl. Climatol.*, 129(1), 1–19, 2017.

857 Jeong, J.-H., Walther, A., Nikulin, G., Chen, D. and Jones, C.: Diurnal cycle of precipitation
858 amount and frequency in Sweden: observation versus model simulation, *Tellus Ser. A Dyn.*
859 *Meteorol. Oceanogr.*, 63(4), 664–674, 2011.

860 Jiao, Y. and Jones, C.: Comparison Studies of Cloud- and Convection-Related Processes
861 Simulated by the Canadian Regional Climate Model over the Pacific Ocean, *Mon. Weather*
862 *Rev.*, 136(11), 4168–4187, 2008.

863 Jones, C., Giorgi, F. and Asrar, G.: The Coordinated Regional Downscaling Experiment:
864 CORDEX--an international downscaling link to CMIP5, *CLIVAR exchanges*, 16(2), 34–40, 2011.

865 Jones, C. G., Willén, U., Ullerstig, A. and Hansson, U.: The Rossby Centre Regional
866 Atmospheric Climate Model part I: model climatology and performance for the present climate
867 over Europe, *Ambio*, 33(4-5), 199–210, 2004.

868 Jones, P. W.: First- and Second-Order Conservative Remapping Schemes for Grids in Spherical
869 Coordinates, *Mon. Weather Rev.*, 127(9), 2204–2210, 1999.

870 Kalognomou, E.-A., Lennard, C., Shongwe, M., Pinto, I., Favre, A., Kent, M., Hewitson, B.,
871 Dosio, A., Nikulin, G., Panitz, H.-J. and Büchner, M.: A Diagnostic Evaluation of Precipitation in
872 CORDEX Models over Southern Africa, *J. Clim.*, 26(23), 9477–9506, 2013.

873 Kim, J., Waliser, D. E., Mattmann, C. A., Goodale, C. E., Hart, A. F., Zimdars, P. A., Crichton, D.
874 J., Jones, C., Nikulin, G., Hewitson, B., Jack, C., Lennard, C. and Favre, A.: Evaluation of the
875 CORDEX-Africa multi-RCM hindcast: systematic model errors, *Clim. Dyn.*, 42(5), 1189–1202,
876 2014.

877 Kisembe, J., Favre, A., Dosio, A., Lennard, C., Sabiiti, G. and Nimusiiima, A.: Evaluation of
878 rainfall simulations over Uganda in CORDEX regional climate models, *Theor. Appl. Climatol.*,
879 137(1), 1117–1134, 2019.

880 Kjellström, E., Bärring, L., Gollvik, S., Hansson, U., Jones, C., Samuelsson, P., Ullerstig, A.,
881 Willén, U. and Wyser, K.: A 140-year simulation of European climate with the new version of the
882 Rossby Centre regional atmospheric climate model (RCA3), [online] Available from:
883 <http://www.diva-portal.org/smash/record.jsf?pid=diva2:947602> (Accessed 19 November 2018),
884 2005.

885 Kjellström, E., Bärring, L., Nikulin, G., Nilsson, C., Persson, G. and Strandberg, G.: Production
886 and use of regional climate model projections - A Swedish perspective on building climate
887 services, *Clim Serv*, 2-3, 15–29, 2016.

888 Kjellström, E., Nikulin, G., Strandberg, G., Christensen, O. B., Jacob, D., Keuler, K., Lenderink,
889 G., van Meijgaard, E., Schär, C., Somot, S., Sørland, S. L., Teichmann, C. and Vautard, R.:
890 European climate change at global mean temperature increases of 1.5 and 2 °C above
891 pre-industrial conditions as simulated by the EURO-CORDEX regional climate models, *Earth*

892 System Dynamics, 9(2), 459–478, 2018.

893 Klutse, N. A. B., Sylla, M. B., Diallo, I., Sarr, A., Dosio, A., Diedhiou, A., Kamga, A., Lampetey, B.,
894 Ali, A., Gbogbaniyi, E. O., Owusu, K., Lennard, C., Hewitson, B., Nikulin, G., Panitz, H.-J. and
895 Büchner, M.: Daily characteristics of West African summer monsoon precipitation in CORDEX
896 simulations, *Theor. Appl. Climatol.*, 123(1), 369–386, 2016.

897 Koenigk, T., Berg, P. and Döscher, R.: Arctic climate change in an ensemble of regional
898 CORDEX simulations, *Polar Res.*, 34(1), 24603, 2015.

899 Kotlarski, S., Lüthi, D. and Schär, C.: The elevation dependency of 21st century European
900 climate change: an RCM ensemble perspective, *Int. J. Climatol.*, 35(13), 3902–3920, 2015.

901 Laprise, R.: Regional climate modelling, *J. Comput. Phys.*, 227(7), 3641–3666, 2008.

902 Legates, D. R. and Willmott, C. J.: Mean seasonal and spatial variability in global surface air
903 temperature, *Theor. Appl. Climatol.*, 41(1), 11–21, 1990.

904 Lenderink, G. and Holtslag, A. A. M.: An updated length-scale formulation for turbulent mixing in
905 clear and cloudy boundary layers, *Quart. J. Roy. Meteor. Soc.*, 130(604), 3405–3427, 2004.

906 Liang, X.-Z.: Regional climate model simulation of summer precipitation diurnal cycle over the
907 United States, *Geophys. Res. Lett.*, 31(24), 2033, 2004.

908 Lindstedt, D., Lind, P., Kjellström, E. and Jones, C.: A new regional climate model operating at
909 the meso-gamma scale: Performance over Europe, *Tellus Ser. A Dyn. Meteorol. Oceanogr.*,
910 67(1), doi:10.3402/tellusa.v67.24138, 2015.

911 Lucas-Picher, P., Caya, D., de Elía, R. and Laprise, R.: Investigation of regional climate models'
912 internal variability with a ten-member ensemble of 10-year simulations over a large domain,
913 *Clim. Dyn.*, 31(7), 927–940, 2008.

914 Lucas-Picher, P., Laprise, R. and Winger, K.: Evidence of added value in North American
915 regional climate model hindcast simulations using ever-increasing horizontal resolutions, *Clim.*
916 *Dyn.*, 48(7), 2611–2633, 2017.

917 Masson, V., Moigne, P. L., Martin, E., Faroux, S., Alias, A., Alkama, R., Belamari, S., Barbu, A.,
918 Boone, A., Bouyssel, F., Brousseau, P., Brun, E., Calvet, J.-C., Carrer, D., Decharme, B., Delire,
919 C., Donier, S., Essaouini, K., Gibelin, A.-L., Giordani, H., Habets, F., Jidane, M., Kerdraon, G.,
920 Kourzeneva, E., Lafaysse, M., Lafont, S., Lebeaupin Brossier, C., Lemonsu, A., Mahfouf, J.-F.,
921 Marguinaud, P., Mokhtari, M., Morin, S., Pigeon, G., Salgado, R., Seity, Y., Taillefer, F., Tanguy,
922 G., Tulet, P., Vincendon, B., Vionnet, V. and Volodire, A.: The SURFEXv7.2 land and ocean
923 surface platform for coupled or offline simulation of earth surface variables and fluxes,
924 *Geoscientific Model Development*, 6(4), 929–960, 2013.

925 Moufouma-Okia, W. and Jones, R.: Resolution dependence in simulating the African
926 hydroclimate with the HadGEM3-RA regional climate model, *Clim. Dyn.*, 44(3), 609–632, 2015.

927 Munday, C. and Washington, R.: Systematic Climate Model Rainfall Biases over Southern
928 Africa: Links to Moisture Circulation and Topography, *J. Clim.*, 31(18), 7533–7548, 2018.

929 Nikulin, G., Jones, C., Giorgi, F., Asrar, G., Büchner, M., Cerezo-Mota, R., Christensen, O. B.,
930 Déqué, M., Fernandez, J., Hänsler, A., van Meijgaard, E., Samuelsson, P., Sylla, M. B. and
931 Sushama, L.: Precipitation climatology in an ensemble of CORDEX-Africa regional climate
932 simulations, *J. Clim.*, 25(18), 6057–6078, 2012.

933 Nikulin, G., Lennard, C., Dosio, A., Kjellström, E., Chen, Y., Hänsler, A., Kupiainen, M., Laprise,
934 R., Mariotti, L., Maule, C. F., van Meijgaard, E., Panitz, H.-J., Scinocca, J. F. and Somot, S.: The
935 effects of 1.5 and 2 degrees of global warming on Africa in the CORDEX ensemble, *Environ.
936 Res. Lett.*, 13(6), 065003, 2018.

937 Olsson, J., Berg, P. and Kawamura, A.: Impact of RCM Spatial Resolution on the Reproduction
938 of Local, Subdaily Precipitation, *J. Hydrometeorol.*, 16(2), 534–547, 2015.

939 Panitz, H.-J., Dosio, A., Büchner, M., Lüthi, D. and Keuler, K.: COSMO-CLM (CCLM) climate
940 simulations over CORDEX-Africa domain: analysis of the ERA-Interim driven simulations at
941 0.44° and 0.22° resolution, *Clim. Dyn.*, 42(11), 3015–3038, 2014.

942 Prein, A. F., Gobiet, A., Truhetz, H., Keuler, K., Goergen, K., Teichmann, C., Maule, C. F., Van
943 Meijgaard, E., Déqué, M., Nikulin, G. and Robert, Vautard, Augustin, Colette, Erik, Kjellström,
944 Daniela Jacob: Precipitation in the EURO-CORDEX 0.11° and 0.44° simulations: high
945 resolution, high benefits?, *Clim. Dyn.*, 46(1-2), 383–412, 2016.

946 Räisänen, J., Hansson, U., Ullerstig, A., Döscher, R., Graham, L. P., Jones, C., Meier, H. E. M.,
947 Samuelsson, P. and Willén, U.: European climate in the late twenty-first century: regional
948 simulations with two driving global models and two forcing scenarios, *Clim. Dyn.*, 22(1), 13–31,
949 2004.

950 Rana, A., Nikulin, G., Kjellström, E., Strandberg, G., Kupiainen, M., Hansson, U. and Kolax, M.:
951 Contrasting regional and global climate simulations over South Asia, *Clim. Dyn.*,
952 doi:10.1007/s00382-020-05146-0, 2020.

953 Rummukainen, M.: State-of-the-art with regional climate models, *Wiley Interdiscip. Rev. Clim.
954 Change*, 1(1), 82–96, 2010.

955 Rummukainen, M.: Added value in regional climate modeling, *WIREs Clim Change*, 7(1),
956 145–159, 2016.

957 Rummukainen, M., Räisänen, J., Bringfelt, B., Ullerstig, A., Omstedt, A., Willén, U., Hansson, U.
958 and Jones, C.: A regional climate model for northern Europe: model description and results from
959 the downscaling of two GCM control simulations, *Clim. Dyn.*, 17(5), 339–359, 2001.

960 Samuelsson, P., Jones, C. G., Will'En, U., Ullerstig, A., Gollvik, S., Hansson, U., Jansson, E.,
961 Kjellström, C., Nikulin, G. and Wyser, K.: The Rossby Centre Regional Climate model RCA3:
962 model description and performance, *Tellus Ser. A Dyn. Meteorol. Oceanogr.*, 63(1), 4–23, 2011.

963 Sanchez-Gomez, E. and Somot, S.: Impact of the internal variability on the cyclone tracks
964 simulated by a regional climate model over the Med-CORDEX domain, *Clim. Dyn.*, 51(3),
965 1005–1021, 2018.

966 Sato, T., Miura, H., Satoh, M., Takayabu, Y. N. and Wang, Y.: Diurnal Cycle of Precipitation in

967 the Tropics Simulated in a Global Cloud-Resolving Model, *J. Clim.*, 22(18), 4809–4826, 2009.

968 Schneider, U., Becker, A., Finger, P., Meyer-Christoffer, A., Ziese, M. and Rudolf, B.: GPCC's
969 new land surface precipitation climatology based on quality-controlled in situ data and its role in
970 quantifying the global water cycle, *Theor. Appl. Climatol.*, 115(1), 15–40, 2014.

971 Scinocca, J. F., Kharin, V. V., Jiao, Y., Qian, M. W., Lazare, M., Solheim, L., Flato, G. M., Biner,
972 S., Desgagne, M. and Dugas, B.: Coordinated Global and Regional Climate Modeling, *J. Clim.*,
973 29(1), 17–35, 2016.

974 Shongwe, M. E., Lennard, C., Liebmann, B., Kalognomou, E.-A., Ntsangwane, L. and Pinto, I.:
975 An evaluation of CORDEX regional climate models in simulating precipitation over Southern
976 Africa: CORDEX simulation of rainfall over Southern Africa, *Atmos. Sci. Lett.*, 16(3), 199–207,
977 2015.

978 Sørland, S. L., Schär, C., Lüthi, D. and Kjellström, E.: Bias patterns and climate change signals
979 in GCM-RCM model chains, *Environ. Res. Lett.*, 13(7), 074017, 2018.

980 Sylla, M. B., Giorgi, F., Coppola, E. and Mariotti, L.: Uncertainties in daily rainfall over Africa:
981 assessment of gridded observation products and evaluation of a regional climate model
982 simulation, *Int. J. Climatol.*, 33(7), 1805–1817, 2013a.

983 Sylla, M. B., Diallo, I. and Pal, J. S.: West African Monsoon in State-of-the-Science Regional
984 Climate Models, in *Climate Variability - Regional and Thematic Patterns*, edited by A. Tarhule,
985 InTech., 2013b.

986 Tamoffo, A. T., Moufouma-Okia, W., Dosio, A., James, R., Pokam, W. M., Vondou, D. A.,
987 Fotso-Nguemo, T. C., Guenang, G. M., Kamsu-Tamo, P. H., Nikulin, G., Longandjo, G.-N.,
988 Lennard, C. J., Bell, J.-P., Takong, R. R., Haensler, A., Tchotchou, L. A. D. and Nouayou, R.:
989 Process-oriented assessment of RCA4 regional climate model projections over the Congo Basin
990 under 1.5°C and 2°C global warming levels: influence of regional moisture fluxes, *Clim. Dyn.*,
991 doi:10.1007/s00382-019-04751-y, 2019.

992 Tangang, F., Supari, S., Chung, J. X., Cruz, F., Salimun, E., Ngai, S. T., Juneng, L.,
993 Santisirisomboon, J., Santisirisomboon, J., Ngo-Duc, T., Phan-Van, T., Narisma, G., Singhru, P.,
994 Gunawan, D., Aldrian, E., Sopaheluwakan, A., Nikulin, G., Yang, H., Remedio, A. R. C., Sein, D. and
995 Hein-Griggs, D.: Future changes in annual precipitation extremes over Southeast Asia
996 under global warming of 2°C, *APN Science Bulletin*, 8(1), doi:10.30852/sb.2018.436, 2018.

997 Temperton, C., Hortal, M. and Simmons, A.: A two-time-level semi-Lagrangian global spectral
998 model, *Q.J Royal Met. Soc.*, 127(571), 111–127, 2001.

999 Termonia, P., Fischer, C., Bazile, E., Bouyssel, F., Brožková, R., Bénard, P., Bochenek, B.,
1000 Degrauwe, D., Derková, M., El Khatib, R. and Others: The ALADIN System and its canonical
1001 model configurations AROME CY41T1 and ALARO CY40T1, *Geoscientific Model Development*,
1002 11, 257–281, 2018.

1003 Tiedtke, M.: A Comprehensive Mass Flux Scheme for Cumulus Parameterization in Large-Scale
1004 Models, *Mon. Weather Rev.*, 117(8), 1779–1800, 1989.

1005 Torma, C., Giorgi, F. and Coppola, E.: Added value of regional climate modeling over areas
1006 characterized by complex terrain-Precipitation over the Alps, *J. Geophys. Res. D: Atmos.*,
1007 120(9), 3957–3972, 2015.

1008 Undén, P., Rontu, L., Järvinen, H., Lynch, P. and Calvo, J.: HIRLAM-5 scientific documentation,
1009 SMHI, SMHI, SE-601 76 Norrköping., 2002.

1010 Van der Linden, P. and Mitchell, E., JFB: ENSEMBLES: Climate change and its
1011 impacts-Summary of research and results from the ENSEMBLES project, 2009.

1012 Walther, A., Jeong, J.-H., Nikulin, G., Jones, C. and Chen, D.: Evaluation of the warm season
1013 diurnal cycle of precipitation over Sweden simulated by the Rossby Centre regional climate
1014 model RCA3, *Atmos. Res.*, 119, 131–139, 2013.

1015 Wang, J. and Kotamarthi, V. R.: Downscaling with a nested regional climate model in
1016 near-surface fields over the contiguous United States: WRF dynamical downscaling, *J.*
1017 *Geophys. Res. D: Atmos.*, 119(14), 8778–8797, 2014.

1018 Washington, R., James, R., Pearce, H., Pokam, W. M. and Moufouma-Okia, W.: Congo Basin
1019 rainfall climatology: can we believe the climate models?, *Philos. Trans. R. Soc. Lond. B Biol.*
1020 *Sci.*, 368(1625), 20120296, 2013.

1021 Wu, M., Schurgers, G., Rummukainen, M., Smith, B., Samuelsson, P., Jansson, C., Siltberg, J.
1022 and May, W.: Vegetation-climate feedbacks modulate rainfall patterns in Africa under future
1023 climate change, *Earth System Dynamics*, 7(3), 627–647, 2016.

1024 Wu, M., Schurgers, G., Ahlström, A., Rummukainen, M., Miller, P. A., Smith, B. and May, W.:
1025 Impacts of land use on climate and ecosystem productivity over the Amazon and the South
1026 American continent, *Environ. Res. Lett.*, 12(5), 054016, 2017.

1027 Xue, Y., Janjic, Z., Dudhia, J., Vasic, R. and De Sales, F.: A review on regional dynamical
1028 downscaling in intraseasonal to seasonal simulation/prediction and major factors that affect
1029 downscaling ability, *Atmos. Res.*, 147-148, 68–85, 2014.

1030 Zhang, W., Jansson, C., Miller, P. A., Smith, B. and Samuelsson, P.: Biogeophysical feedbacks
1031 enhance the Arctic terrestrial carbon sink in regional Earth system dynamics, *Biogeosciences*,
1032 11(19), 5503–5519, 2014.

1033